

## Doping of organic semiconductors induced by lithium fluoride/aluminum electrodes studied by electron spin resonance and infrared reflection-absorption spectroscopy

E. D. Głowacki,<sup>1</sup> K. L. Marshall,<sup>2</sup> C. W. Tang,<sup>3,a)</sup> and N. S. Sariciftci<sup>4</sup>

<sup>1</sup>Linz Institute for Organic Solar Cells (LIOS), Johannes Kepler University Linz, Altenberger Straße 69 A-4040, Linz, Austria

<sup>2</sup>Laboratory for Laser Energetics, University of Rochester, 250 East River Road, Rochester, New York 14623, USA

<sup>3</sup>Department of Chemical Engineering, University of Rochester, Rochester, New York 14627, USA

<sup>4</sup>Linz Institute for Organic Solar Cells (LIOS), Johannes Kepler University Linz, Altenberger Straße 69 A-4040, Linz, Austria

(Received 18 May 2011; accepted 7 July 2011; published online 28 July 2011)

We report our investigations on the chemical doping mechanisms induced by LiF|Al electrodes evaporated onto fullerene thin films. Electron spin resonance (ESR) and infrared reflection-absorption spectroscopy (IRRAS) are utilized to characterize C<sub>60</sub>|Al and C<sub>60</sub>|LiF|Al interfaces. ESR spectra show that deposition of LiF followed by Al generates C<sub>60</sub> radical anions and also the presence of an additional paramagnetic species of lower concentration that is present in all C<sub>60</sub> films regardless of LiF. IRRAS clarifies the mechanism occurring at the C<sub>60</sub>|LiF|Al interface, showing that interaction between LiF and C<sub>60</sub> followed by deposition of Al causes LiF clusters to chemically dissociate. © 2011 American Institute of Physics. [doi:10.1063/1.3615799]

Interfaces of metal contacts and organic semiconductors play a crucial role in the performance of organic electronic devices. Efficient electroluminescent and photovoltaic diodes require Ohmic anode and cathode contacts. In the case of electron injecting/extracting contacts, a low work function metal is required to align with the electron-conducting level (lowest unoccupied molecular orbital, LUMO) of the electron-transport layer in these devices. A commonly used technique to avoid problematic low work function metals is to deposit a thin (0.5- to 2-nm) layer of LiF onto the electron-transport layer prior to depositing aluminum as the electrode metal.<sup>1,2</sup> Ohmic contact behavior has been reported for C<sub>60</sub> as the electron-transport layer with LiF|Al (Ref. 3) as the electrode. Several mechanisms for improved electron injection have been proposed: enhanced electron tunneling from Al through the thin LiF layer,<sup>1,4</sup> chemical reactions causing n-doping of the electron-transport layer,<sup>5,6</sup> dipole alignment,<sup>7</sup> and shielding of the organic layers from detrimental reactions with aluminum metal,<sup>1,4</sup> among others. Here we present results showing that in the case of C<sub>60</sub>|LiF|Al, upon deposition of Al, n-doping of C<sub>60</sub> occurs via LiF dissociation and formation of a C<sub>60</sub><sup>-</sup>Li<sup>+</sup> charge-transfer complex. We employ electron spin resonance (ESR) to probe paramagnetic species in C<sub>60</sub> films and infrared reflection-absorption spectroscopy (IRRAS) to clarify the mechanism LiF dissociation. The overall reaction scheme that we propose is as follows: 3C<sub>60</sub> + 3LiF + Al → 3(C<sub>60</sub><sup>-</sup>Li<sup>+</sup>) + AlF<sub>3</sub>.

Thin-film samples were prepared by thermal deposition under vacuum (1 × 10<sup>-6</sup> Torr). All annealing processes were conducted in N<sub>2</sub> atmosphere (<1 ppm O<sub>2</sub>). Samples were exposed to air during characterization experiments, all of which were conducted at room temperature. Film thicknesses

were kept identical for all samples: 35 nm of C<sub>60</sub>, 2 nm of LiF, and 150 nm of Al. For ESR measurements, films of area 1.65 cm<sup>-2</sup> were deposited on substrates cut from single-crystalline quartz. Quartz was chosen to avoid paramagnetic impurities present in common borosilicate glass. Spectra were obtained using a Bruker ESP300E X-band instrument equipped with a TM110 resonator cavity. The sample was placed in the nodal plane of the electric field to prevent the metal layer from interfering with the resonator mode. Quantitative spin populations were calculated on the basis of a NIST Al<sub>2</sub>O<sub>3</sub>:Cr standard. All thin-film samples for the IRRAS experiments were deposited onto glass slides with 260 nm of Al serving as the reflection element. For top-deposited Al, a film thickness of 2 nm was used. Spectra, averaged over 500 scans with 4 cm<sup>-1</sup> resolution, were obtained using a grazing-angle reflectance accessory for the Bruker Hyperion IR microscope equipped with a Mercury Cadmium Telluride detector cooled by liquid N<sub>2</sub>.

Several paramagnetic species have been detected in OLED devices using ESR, including charge carriers in the form of hopping radical anions and cations, triplet excitons, and permanently charged paramagnetic impurities.<sup>8</sup> In this study, we evaluated C<sub>60</sub> films with Al and Al/LiF as the electrode contact to probe reactivity of LiF with C<sub>60</sub>. Films of neat C<sub>60</sub>, Al on C<sub>60</sub>, and LiF/Al on C<sub>60</sub>, as well as films of opposite deposition order, that is, C<sub>60</sub> on Al, C<sub>60</sub> on LiF/Al, were investigated. Two types of paramagnetic species were observed. In neat C<sub>60</sub> and Al on C<sub>60</sub> films, an ESR signal at g = 2.001 is observed. This same 2.001 signal is also observed in films of C<sub>60</sub> on Al and C<sub>60</sub> on LiF/Al. Annealing at 120 °C in all cases causes an increase in the 2.001 signal by about 25%. Annealing at higher temperatures up to 280 °C does not appreciably affect the 2.001 signal strength. Figure 1 shows the ESR spectra obtained for samples with both deposition orders. Assuming that the paramagnetic

<sup>a)</sup>Author to whom correspondence should be addressed. Electronic mail: ching.tang@rochester.edu.

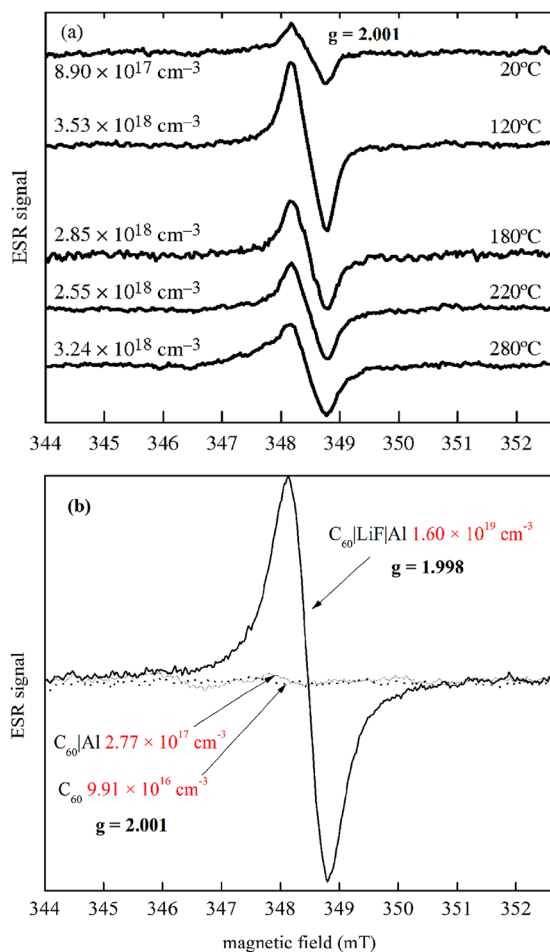


FIG. 1. (Color online) (a) Electron spin resonance (ESR) of Al|LiF|C<sub>60</sub> (inverted deposition sequence) samples annealed at different temperatures. Only a signal for  $g = 2.001$  is detected. (b) ESR signal of 35-nm C<sub>60</sub> neat film, and with Al and LiF/Al electrodes deposited on top. Films with LiF demonstrate a strong signal with a  $g$ -value of 1.998, corresponding to the C<sub>60</sub>-radical anion, while the remaining samples show a  $g = 2.001$  signal.

species corresponding to the  $g = 2.001$  signal resides in the C<sub>60</sub> layer, the population is estimated to be 0.005 to 0.01 mol. % of the total C<sub>60</sub> film. This radical signal has been reported in powder C<sub>60</sub> samples under vacuum and was found to increase reversibly with the presence of oxygen.<sup>9</sup> A  $g$ -value of 2.001 is characteristic of a weakly-bound carbon based radical and is too low for an oxygen-centered radical,<sup>10</sup> suggesting a C<sub>60</sub>-oxygen adduct with a cage-centered radical.

For LiF/Al on C<sub>60</sub> films, however, the deposition of LiF followed by Al resulted in the appearance of an ESR signal with  $g = 1.998$  corresponding to the C<sub>60</sub> radical anion. This  $g$ -value is in excellent agreement with prior ESR studies of photoexcited C<sub>60</sub> films.<sup>11</sup> Assuming that the C<sub>60</sub> radical anions are uniformly distributed throughout the C<sub>60</sub> film, we calculate a concentration of 1 to  $2 \times 10^{19}$  cm<sup>-3</sup>, which is about 1 mol. %. The data strongly suggest that the radical anions are associated with the C<sub>60</sub><sup>-</sup>Li<sup>+</sup> charge-transfer complexes. It is conceivable, however, that the concentration of the complexes can be much higher near the LiF/Al electrode. Annealing of this sample does not change the amount of ESR signal. In contrast, the  $g = 1.998$  signal is not observed in films of C<sub>60</sub> deposited on LiF/Al, even with thermal

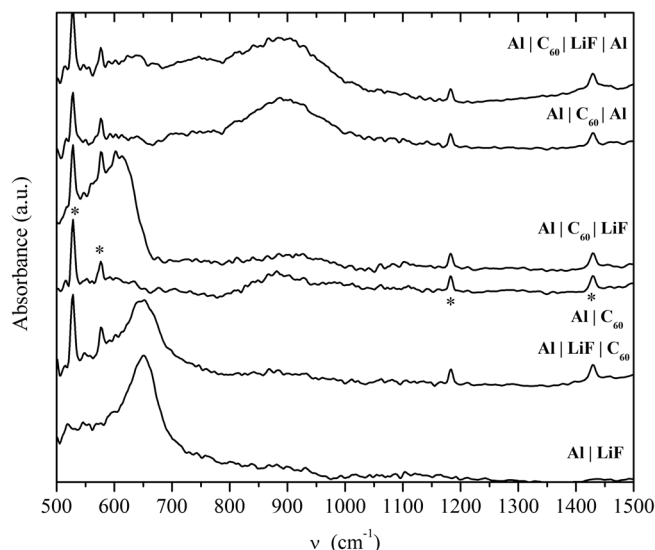


FIG. 2. IRRAS spectra of LiF, C<sub>60</sub>, and LiF/Al with different deposition orders. The spectra are offset for clarity. A 260-nm Al film serves as the bottom reflection element in all cases. Asterisks mark the four vibrational modes of C<sub>60</sub>.

annealing up to 280 °C. These observations show that the deposition sequence with LiF deposited on top of C<sub>60</sub> followed by Al is integral for LiF to be effective in forming the C<sub>60</sub><sup>-</sup>Li<sup>+</sup> complexes. Over a dozen measured samples, the standard deviation in the population of the  $g = 2.001$  species is small,  $\pm 2.3 \times 10^{17}$  cm<sup>-3</sup> for samples with C<sub>60</sub> as the upper (exposed) layer, and  $\pm 2.0 \times 10^{16}$  cm<sup>-3</sup> for samples with C<sub>60</sub> covered with Al. The standard deviation for the population of the C<sub>60</sub> radical anion ( $g = 1.998$ ) is much higher,  $\pm 1.9 \times 10^{19}$  cm<sup>-3</sup>.

In order to probe the reaction occurring when LiF and Al are deposited onto C<sub>60</sub>, we utilized IRRAS at a grazing angle. This method relies on constructive interference of  $p$ -polarized light at the metal interface at grazing angle to produce amplified absorption by dipoles aligned perpendicular to the metal surface.<sup>12</sup> Figure 2 shows the results for IRRAS: a 2-nm film of LiF on Al (260 nm), denoted Al/LiF in the figure, deposited on glass substrates furnished a well-resolved peak between 600 and 660 cm<sup>-1</sup>, corresponding<sup>13</sup> to the longitudinal optical (LO) phonon of LiF clusters. Likewise, a 35 nm film of C<sub>60</sub> on Al, Al/C<sub>60</sub>, provided four well-resolved and clearly visible peaks attributable to C<sub>60</sub>, despite the fact that C<sub>60</sub> vibrational modes are known to be weak. The C<sub>60</sub> on LiF film and Al/LiF/C<sub>60</sub> produced spectra that were a superposition of LiF and C<sub>60</sub> individual films. In contrast, Al/C<sub>60</sub>/LiF film obtained by reversing the deposition order resulted in a red shift of the LiF LO peak at 650 cm<sup>-1</sup> by 40 cm<sup>-1</sup> to 610 cm<sup>-1</sup>.

Also shown in Figure 2 are IRRAS spectra of 2 nm of Al on C<sub>60</sub>, Al/C<sub>60</sub>/Al (2 nm) and on C<sub>60</sub>/LiF, Al/C<sub>60</sub>/LiF/Al (2 nm). The spectrum of Al/C<sub>60</sub>/Al (2 nm) is practically identical that of Al/C<sub>60</sub>, indicating the deposition of 2 nm of Al has no effect on C<sub>60</sub>. However, the deposition of 2 nm Al on C<sub>60</sub>/LiF, Al/C<sub>60</sub>/LiF/Al (2 nm), causes the red-shifted LiF peak at 610 cm<sup>-1</sup> to disappear altogether. This disappearance indicates that the LiF is completely dissociated or the phonon resonance is shifted to a frequency lower than 500

$\text{cm}^{-1}$ , below the MCT detection limit. The LO mode in alkali halides is always at a higher frequency than the transverse optical (TO) mode.<sup>13,14</sup> This is due to strong polarization created by vibrating ions which produces an electric field that assists the elastic restoring force of the LO mode but opposes that of the TO mode, causing LO and TO modes to split. This splitting is known to be sensitive to crystallite size and interface effects. Small crystallites lower the frequency of the LO mode.<sup>15</sup> The disappearance of the  $610 \text{ cm}^{-1}$  LiF peak is consistent with dissociation of the LiF layer into smaller clusters or reactions that produce  $\text{Li}^+\text{C}_{60}^-$  complexes. Both would result in the disappearance of the LO peak. Additionally, we observed that deposition of Al onto neat LiF films produced no changes in the LO mode. These observations preclude the possibility that the LiF layer is acting as an insulator in LiF/Al contacts in OLED and photovoltaic devices, consistent with prior reports.<sup>3</sup> IRRAS however does not allow us to determine where  $\text{F}^-$  ions go upon dissociation of LiF. Formation of highly stable  $\text{AlF}_3$  has been proposed as a mechanism.<sup>17</sup>  $\text{AlF}_3$ , which has a broad and weak absorption between  $600$  and  $700 \text{ cm}^{-1}$  (Ref. 16), is unlikely to be distinguishable in our IRRAS spectra. The four fundamental modes of  $\text{C}_{60}$  remain unchanged for Al/ $\text{C}_{60}$ /LiF/Al (2 nm), suggesting that any polymerization or other symmetry-lowering reactions<sup>18</sup> are not detectable.

Our results are in agreement with the reaction model that LiF, deposited onto the fullerene films, forms clusters, but does not interact with the underlying  $\text{C}_{60}$ , whereas aluminum atoms, deposited on the LiF clusters, cause the breakup of the clusters and reaction with  $\text{C}_{60}$  to form  $\text{C}_{60}^-\text{Li}^+$ .

This work was supported by the European Science Foundation (ESF) and the U.S. Department of Energy Office of Inertial Confinement Fusion under Cooperative Agreement No. DE-FC52-08NA28302, the University of Rochester, and the

New York State Energy Research and Development Authority. Work at Johannes Kepler University Linz was performed within the Nationales Forschungsnetzwerk (NFN) "Interface controlled and functionalised organic thin films" from the Austrian Foundation for Advancement of Scientific Research (FWF S 9711-N20). The support of DOE does not constitute an endorsement by DOE of views expressed in this article. We warmly thank Thomas Pawlik for assistance in quantifying the ESR signal and fruitful discussions.

- <sup>1</sup>L. S. Hung, C. W. Tang, and M. G. Mason, *Appl. Phys. Lett.* **70**, 152 (1997).
- <sup>2</sup>G. E. Jabbour, B. Kippelen, N. R. Armstrong, and N. Peyghambarian, *Appl. Phys. Lett.* **73**, 1185 (1998).
- <sup>3</sup>X. D. Feng, C. J. Huang, V. Lui, R. S. Khangura, and Z. H. Lu, *Appl. Phys. Lett.* **86**, 143511 (2005).
- <sup>4</sup>T. M. Brown, R. H. Friend, I. S. Millard, D. J. Lacey, J. H. Burroughes, and F. Cacialli, *Appl. Phys. Lett.* **77**, 3096 (2000).
- <sup>5</sup>Q.-T. Le, L. Yan, Y. Gao, M. G. Mason, D. J. Giesen, and C. W. Tang, *J. Appl. Phys.* **87**, 375 (2000).
- <sup>6</sup>J. Kido and T. Matsumoto, *Appl. Phys. Lett.* **73**, 2866 (1998).
- <sup>7</sup>M. A. Baldo and S. R. Forrest, *Phys. Rev. B* **64**, 085201 (2001).
- <sup>8</sup>T. D. Pawlik, M. E. Kondakova, D. J. Giesen, J. C. Deaton, and D. Y. Kondakov, *J. Soc. Inf. Disp.* **17**, 279 (2009).
- <sup>9</sup>M. D. Pace, T. C. Christidis, J. J. Yin, and J. Milliken, *J. Phys. Chem.* **96**, 6855 (1992).
- <sup>10</sup>M. Mermoux, Y. Chabre, and A. Rousseau, *Carbon* **29**, 469 (1991).
- <sup>11</sup>V. Dyakonov, G. Zorinians, M. Scharber, C. J. Brabec, R. A. J. Janssen, J. C. Hummelen, and N. S. Sariciftci, *Phys. Rev. B* **59**, 8019 (1999).
- <sup>12</sup>F. M. Mirabella, *Modern Techniques in Applied Molecular Spectroscopy* (Wiley, New York, 1998).
- <sup>13</sup>M. Gottlieb, *J. Opt. Soc. Am.* **50**, 343 (1960).
- <sup>14</sup>R. H. Lyddane, R. G. Sachs, and E. Teller, *Phys. Rev.* **59**, 673 (1941).
- <sup>15</sup>C. Kittel, *Introduction to Solid State Physics*, 3rd ed. (Wiley, New York, 1966).
- <sup>16</sup>W. J. H. van Gennip, J. K. J. van Duren, P. C. Thüne, R. A. J. Janssen, and J. W. Niemantsverdriet, *J. Chem. Phys.* **117**, 5031 (2002).
- <sup>17</sup>C. Alonso, A. Morato, F. Medina, F. Guirado, Y. Cesteros, P. Salagre, J. E. Sueriras, R. Terrado, and A. Giralt, *Chem. Mater.* **12**, 1148 (2000).
- <sup>18</sup>G. Cardini, R. Bini, P. R. Salvi, V. Schettino, M. L. Klein, R. M. Strongin, L. Brard, and A. B. Smith, *J. Phys. Chem.* **98**, 9966 (1994).